Characterization of Electron Beam Irradiated Poly Vinyl Alcohol / Poly Ethylene Glycol Blends

Z. I. Ali[*1] and W.H. Essa[2]

[1]National Center for Radiation Research and Technology (NCRRT), P.O. Box 29 Madinat Nasr, Nasr City, Cairo, Egypt

[1]Department of Spectroscopic, Physics Division, National Research Center, Giza, 12622, Egypt

Abstract

Poly vinyl alcohol (PVA) and poly ethylene glycol (PEG) blends were prepared and irradiated with different electron beam irradiation doses. The influence of the irradiation dose, and PEG content on the physico-chemical properties was investigated. The data regarding gel content demonstrated that the radiation-induced crosslinking of PVA and PVA/PEG samples increased as a result of increasing irradiation dose and decreasing PEG content. The swelling volume ratio shows an opposite behavior. The XRD parameters (crystllinity percent and d-spacing values) show a decreasing behavior for PVA and PVA/PEG blends as a result of either irradiation or blending PVA matrix with PEG. The DSC data illustrate a decreasing trend in melting point, glass transition temperature, and degree of crystallinity with increasing irradiation dose or PEG content.

1. Introduction

Poly vinyl alcohol (PVA) is a commercial polymer and its properties depend on its molecular weight, total degree of hydrolysis, sequence distribution of monomer units, and tacticity. PVA is a semicrystalline polymer and its crystalline index depends on the synthetic process and physical ageing. Hydrogen bonds keep together polymer chains, even in the amorphous phase. PVA has been the subject of intensive research because it has many applications in industry and it is of relatively low cost [1-6].

Poly ethylene glycol (PEG) is a hydrophilic, nontoxic, water soluble polymer and has a wide range of applications, mostly in cosmetic industries. This is because it dose not cause damage when it comes in contact with the skin or lips [7]. PEG has thermal stability

---

[*]*Corresponding author*: zakariaismaiel30@yahoo.com

and unhydrolyzation properties, which makes it more environmentally friendly. In addition, PEG is more common which could reduce the cost of experiments and simplify the experiments process. PVA and PEG blends have been widely explored as water soluble polymers for numerous industrial, biomedical and pharmaceutical applications due to the advantages of nontoxic, non-carcinogenic and bioadhesive properties [8].

The miscibility between the constituents of a polymer mixture is an important factor in the development of new materials based on polymeric blends. In miscible polymeric blends, there are often specific interactions between functional groups or polymer segments that lead to decrease of the Gibbs energy of mixing. Miscible polymer blends present only one phase, while immiscible blends present separated domains, and the final properties of polymer blends are directly related to the degree of their miscibilities [9]. In immiscible polymer blends, their physical properties are poor compared with those of parent polymers because of phase separations arising from weak interaction at the boundaries of component polymers. The miscibility and the physical properties of polymer blends can be improved by applying intermolecular interaction such as hydrogen bonding and dipole-dipole interaction between blend components. Intermolecular hydrogen bonding interaction by hydroxyl, halogen, carbonyl, and amide groups leads to the improvement of miscibility based on favorable enthalpic interaction between polymer chains. Addition of compatibilizer into immiscible polymer blends also improves the miscibility and the physical properties [6, 9-12]. For polymer-polymer miscibility investigations, the most useful techniques are electronic microscopy [13], spectroscopy [14], and thermal analysis [15]. Electron beam irradiation of polymer blends has been employed in improving the properties and miscibility of blends. High energy irradiation produces free radicals that can readily interact with each other forming crosslinking and strengthening the polymer structure. The objective of this study is to determine the effect of electron beam irradiation on the structural, physical and chemical properties of water soluble polymer blends based on PVA and PEG.

2. Experimental

2.1. *Materials*

PVA (M. wt. = 35000 g/mol) was obtained from Laboratory Rasayan, Cairo, Egypt. It was in the form of powder, partially hydrolyzed. PEG was of laboratory grade, had an average molecular weight of 6000-7500 g/mol, melting point of 56-61°C and was purchased from El-Nasr pharmaceutical Chemicals Co., Egypt.

2.2. *Sample preparation*

Polymer blend films were prepared using solvent casting technique. The total amount of the dissolved solid polymers is kept constant, (3 gm), in all of prepared samples. PVA/PEG blends of different ratios (100/0.0, 95/5, 90/10, 85/15 and 80/20 gm,

respectively) were prepared as follow: an accurate weight of PVA is dissolved in 30 ml of distilled water at 60-70°C with stirring for about 6 h until clear solution is obtained. The solution is left to cool at ambient condition while stirring and thereafter PEG is added with continuous stirring for about 2 h to insure a homogenous solution. Finally, the polymer solution was casted on a 15×15 cm glass plate, left to dry in air to form the desired film.

2.3. Irradiation process

Electron beam (EB) irradiation was carried out in atmospheric air at ambient temperature using 1.5 MeV and 25 Kw electron beam accelerator. All samples were irradiated on one side using a current of 10 mA and scan width variable up to 90 cm. The polymeric samples were exposed to an irradiation dose of about 5 kGy each pass. Several passes under these conditions were required for high irradiation doses. The irradiation doses are ranged throughout this work from 25 to 100 kGy.

2.4. *Characterization*

2.4.1. *Swelling behavior and gel content of polymeric samples*

Polymeric films were cut into pieces of 2 × 2 cm and then accurately weighed (W_1), which were then placed into 500 ml glass containers filled with distilled water. The solvent containing samples are stored for 24 hours at room temperature. The swollen samples were removed and superficial moisture was removed using filter paper, the weight of the deswollen sample was determined immediately, (W_2). Thereafter, the samples were dried in an oven at 40-50°C until a constant weight was reached, (W_3). The water swelling ratio (wt %), soluble fraction (s), and gel content (g %), were calculated as follows:

Swelling ratio % = $\{(W_2 - W_1) / W_1\} \times 100$ (1)

$s = (W_1 - W_3) / W_1$ (2)

g % = $(W_3 / W_1) \times 100$ (3)

2.4.2. *Fourier transform infra red (FTIR) spectroscopy*

FTIR spectrometry (ATI Mattson, Genesis series, USA) was used for scanning and measuring the absorption spectra. The spectra of unirradiated and irradiated samples were measured using a designed holder for sample of 2 × 2 cm dimension, over the range 400-4000 cm^{-1}.

2.4.3. *X-ray diffraction (XRD)*

X-ray diffraction (XRD) patterns of polymeric blends were recorded by using a Philips X-ray diffractometer (PW 13900), using Cu-K$_\alpha$ ($\lambda = 1.5418$ Å) as incident radiation.

2.4.4. *Differential scanning calorimetery (DSC)*

DSC used here is of the type DSC-50 instrument from Shimadzu, Japan. The sample films were first cooled to -110°C and the DSC thermograms were then recorded at a heating rate of 10°C/min from -110 up to 250°C under atmosphere of nitrogen. The heat required for melting of a sample (heat of fusion, ΔH_m) was determined by integrating the area under the melting peak over the range 190-240°C. ΔH_m value was corrected for the residual water present in the investigated sample by also analyzing the peak representing the heat required for the evaporation of water (at approximately 100°C). By comparing the area under water peak (ΔH_{water}) which is the heat required to evaporate water from the sample, to the heat of vaporization of water (ΔH_{vap}), the total amount of water in sample was calculated as follow:

$$\text{Weight of water in sample} = \Delta H_{water} \times W_s / \Delta H_{vap} \qquad (4)$$

where W_s is the sample weight.

The degree of crystallinity (X_c) based on dry PVA volume, was calculated by dividing the corrected ΔH_m by the heat required for melting a 100% crystalline PVA sample ($\Delta H_{100} = 138.6$ J/g) according to the following equation [16-17]

$$X_c \text{ (in \%)} = (\Delta H_m / \Delta H_{100}) \times 100 \qquad (5)$$

For PVA//PEG blend, the weight of PEG was subtracted from the total sample weight when calculating the degree of crystallinity.

3. Results and Discussion

3.1. *Swelling behavior and gel content*

A characteristic property of network structure of polymeric materials is their ability to swell in suitable solvents. If a network structure is immersed in a solvent that is miscible with the polymer chains of polymer network, the solvent are imbibed, and the polymer network swells [18]. Degree of swelling of polymer gels significantly depends on the environment such as the nature of swelling solvents, temperature etc. which influence thermodynamic interactions between the constituent of polymer blend and solvent. PVA became insoluble in water for a sufficiently large degree of crosslinking. The swelling, and gel content of samples were used as a measure of polymer crosslink density.

The swelling ratio of PVA and PVA/PEG samples, at room temperature, is plotted against irradiation in Fig. 1. The data revealed that swelling ratio gradually decreases with

increase of irradiation dose, indicating an increase in crosslink density of irradiated samples, which make polymer chain more rigid and compact. This behavior reduces the average chain length between crosslinks, restricting chain motion and extension. Volumetric expansion of polymeric network decreases as a function of increasing crosslink density. It was also observed that increasing PEG content into polymer blends increases the swelling ratios, and this is due to the increment in PVA hydrophilicity. In addition, it can be seen that the level of increase in swelling ratio (30, 25, 20, and 15 %) decreases with increasing PEG content (5, 10, 15, and 20 %). PEG is more hydrophilic than PVA so the swelling ratio increased with an increase in the molar ratio of hydrophilic groups of PEG component.

A major practical use of high energy radiation is to modify crosslink density of polymeric materials. Generally, the extent of radiation induced crosslinking of polymers can be estimated from gel content determination [19-20]. Thus, in order to elucidate radiation induced crosslinking, gel content of investigated samples was determined as a function of irradiation dose and the results were plotted in Fig. 2. Apparently, it was observed that gel content increases with increasing irradiation dose. This can be attributed to the formation of a three dimensional network structure upon irradiation. Furthermore, another factor which has a great effect on gel content is the PEG content. One can see that gel content decreased markedly with increasing of PEG content.
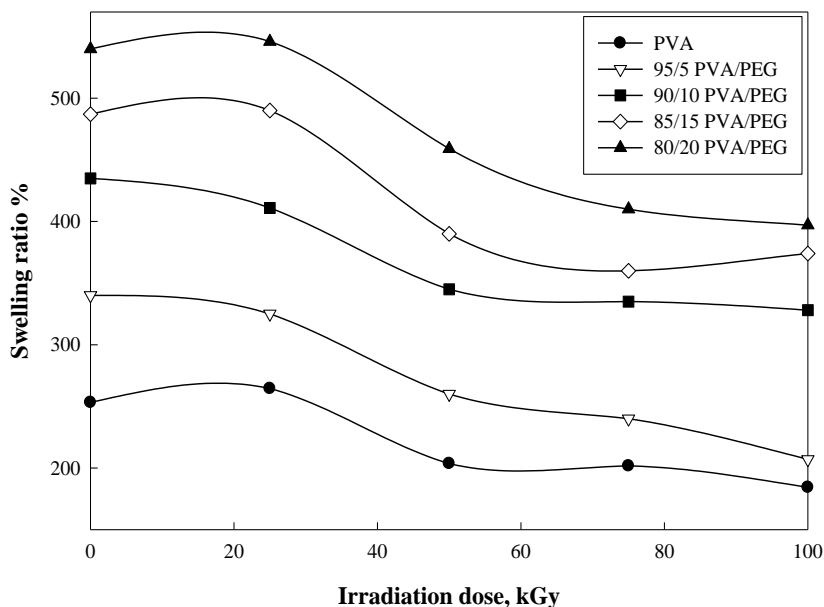

Fig. 1. Change in swelling ratio percent against irradiation dose for PVA and PVA/PEG blends with different PEG contents.
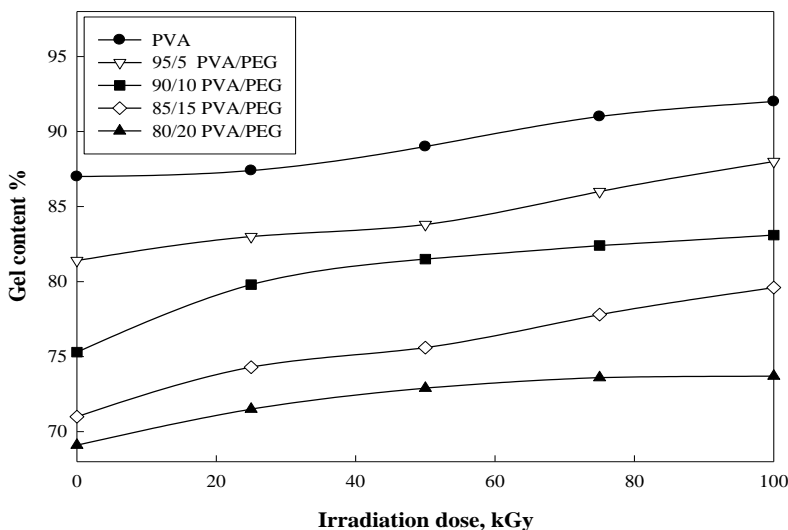
Fig. 2. Gel content % as a function of irradiation dose for PVA and PVA/PEG blends with different PEG contents.

On the basis of the results obtained regarding gel content, the following conclusions have been drawn:

1. The gel content (i.e., crosslink density) markedly increased with the increase of irradiation dose. This can be attributed due to the formation of a three dimensional network structure upon irradiation.

2. The maximum gel content (g_{max} %) values gradually decreased with increasing PEG content (Table 1)

Table 1. The maximum gel content (g_{max} %) of PVA and PVA/PEG samples.

Composition	g_{max} %
PVA	92.6
PVA/PEG (95/5 wt%)	88.2
PVA/PEG (90/10 wt%)	83.8
PVA/PEG (85/15 wt%)	80.0
PVA/PEG (80/20 wt%)	74.5

3.2. *Fourier transform infra red (FTIR) spectroscopic investigation*

Fourier transform infrared (FTIR) spectroscopy is one of the most powerful spectroscopic techniques to investigate polymeric systems because it provides information for both blend

composition and polymer-polymer interactions using those vibrational modes attributed to ''free'' and hydrogen bonded of hydroxyl and carbonyl groups [9]. Hydrogen bonding and/or other secondary interactions between functional groups on dissimilar polymers should theoretically cause a shift in peak position of the participating groups. This behavior is exhibited by miscible polymer blends that show extensive phase mixing. Hydrogen bonding interactions usually shift stretching frequencies of the participating groups towards lower wave-number usually with increased peak intensity and broadening, and the shift in peak position will depend on the strength of the interaction [21].

The representative FTIR spectra of unirradiated PVA and PVA/PEG blends are shown in Fig. 3. The O-H stretching band in FTIR spectrum is by far the most characteristic feature of alcohols and phenols. PVA sample gave broad band centered at 3300 cm^{-1} as the stretching vibration of hydroxyl group with strong hydrogen bonding as intra- and/or inter type, [22-23]. The shoulder absorption peak at 3556 cm^{-1} is associated with free hydrogen boding O-H stretching. Two strong peaks at 2990 and 2840 cm^{-1} are the characteristic bands of asymmetric and symmetric C–H stretching respectively. The stretching vibrational bands of C = O and C = C groups appeared at 1650 and 1560 cm^{-1}, respectively. The C = O bands were attributed to the carbonyl functional groups due to the residual acetate groups remaining after the manufacture of PVA from hydrolysis of poly (vinyl acetate) or oxidation during manufacturing and processing [24]. The values of C = O and/or C = C peak intensities indicate that PVA have the same resonating structure from alkene↔alkane and C = O↔C-O$^-$ and/or presence of hydrogen bond with oxygen of C = O group [25]. The absorption band at 1436 cm^{-1} is assigned as CH$_2$ bending vibration while the deformation vibration of C–CH$_3$ is associated with the absorption band at 1348 cm^{-1}. A signal at 1211 cm^{-1} is due to CH$_2$ wagging and that at 1133 cm^{-1} is assigned as C–C and C–O–C stretching vibrations [26-28].
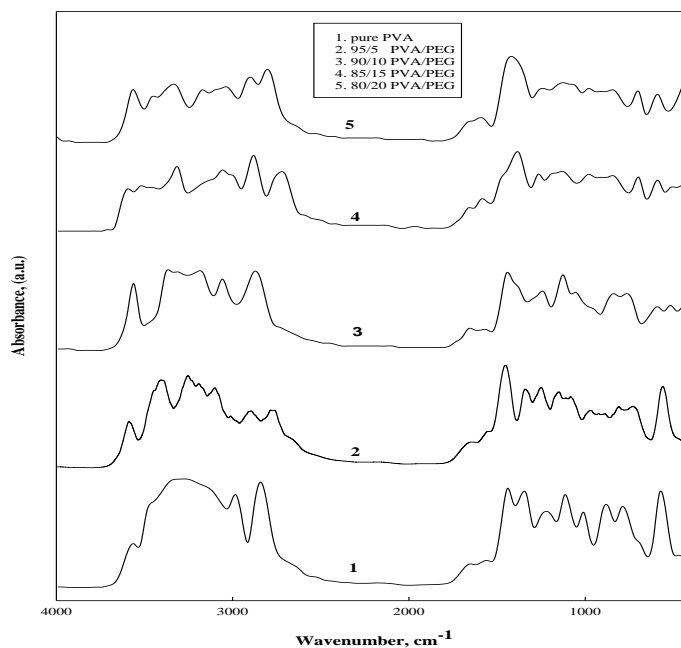

Fig. 3. FTIR spectrum of unirradiated PVA and PVA/PEG blends with different PEG contents.

In Fig. 3, it can be seen that the spectra of PVA/PEG blends showed a good resolution of 3300 cm^{-1} band, i.e., blending of PVA with PEG shows a significant splitting was observed in the OH stretching vibration. In contrast to control PVA and distinguishing between H-bonded and non-H-bonded of hydroxyl groups, PVA/PEG blends show clear demarcation. An intense absorption peak at 2724 cm^{-1} assigned for C-H stretching was appeared at high content of PEG component. As PEG content increases, the intensity of the absorption band at 1650 cm^{-1} was increased whereas the intensity of the absorption peak at 1560 cm^{-1} decreases markedly. The intensity of C-H stretching band at 1348 was found to decrease with increasing PEG content until it becomes weak shoulder or confused with the peak at the 1438 cm^{-1}. The vibrational bands in the spectral region 650-1300 cm^{-1}, showed decreasing tendency and shifted to higher wave-numbers. The intensity of the absorption band at 1133 cm^{-1} was decreased markedly as a result of increasing PEG content reflecting a negative role of PEG component on crystalline nature of the PVA.
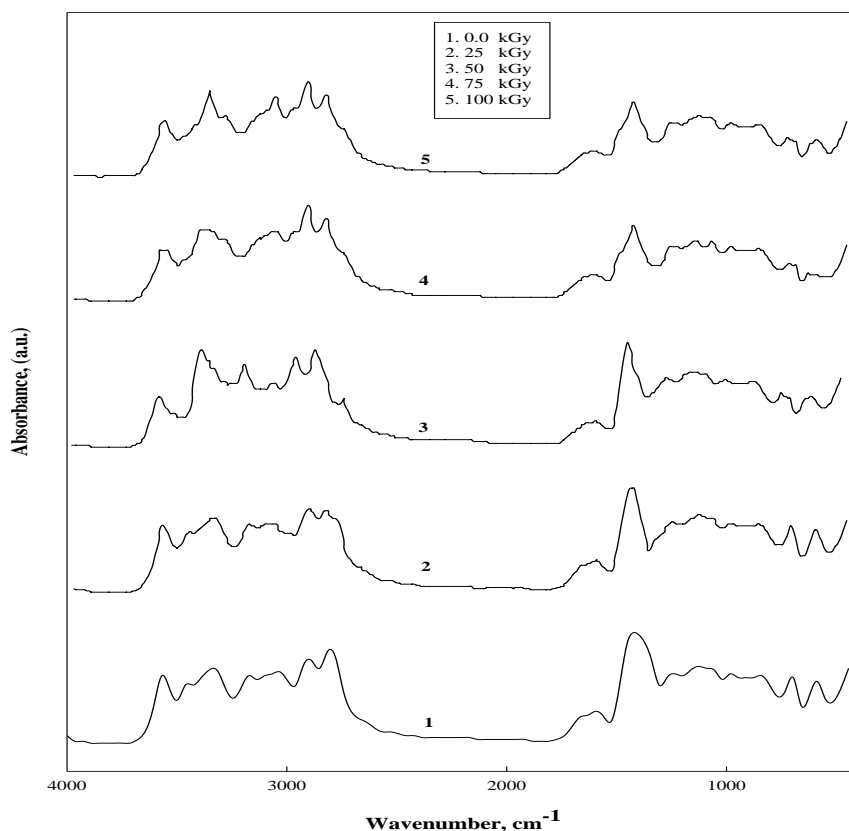

Fig. 4.   FTIR spectrum of 80/20 PVA/PEG (85/15 wt%) blend irradiated with various irradiation doses.

PVA has a strong tendency to form hydrogen bonding as well as with other species containing highly electronegative groups. PEG has electronegative oxygen and hydroxyl groups, which can assist its miscibility with PVA. In contrast, our experimental observations reflect the occurrence of some kind of phase separation. This can be understood as follow: all of the hydroxyl bands could be resolved into ''free'' hydroxyl peaks (free hydrogen bonding) ranging from 3450 to 3550 cm^{-1}, and associated'' hydrogen bonded hydroxyl peak ranging from 3300 to 3450 cm^{-1}, which is attributed to a wide distribution of hydrogen bonded hydroxyl stretching frequencies. The hydroxyl group of pure PVA appeared mostly on the hydrogen bonded configuration, corresponding to PVA containing a high density hydroxyl group and more flexible opportunity to form intra-molecular hydrogen bonding. On the other hand, the hydroxyl group of PEG is favorable for the free hydrogen bonding since PEG merely contains a hydroxyl group on the end chain with less opportunity to form the intra- and/or intermolecular hydrogen bonding within PEG chains or with PVA matrix [29]. The red shift in the position of the hydroxyl group vibrational bands supports our prediction of weak hydrogen bonding interaction between the two polymers. Fig. 4 shows the FTIR spectrum of irradiated PVA/PEG (85/15 wt%) blends with various irradiation doses (25-100 kGy). Here, there is no remarkable change as a result of irradiation, except smoothing of peaks in the spectral region 1380-500 cm^{-1}.

3.3. *X-ray diffraction analysis*

X-ray diffraction analysis of PVA samples was used to determine the variations in structure and crystallinity percent as a result of different treatments such as blending of PVA with PEG and irradiation. XRD patterns of unirradiated pure PVA and unirradiated PVA/PEG (90/10 wt%) blends are presented in Fig. 5. The diffraction pattern of PVA sample at 11.5°, 14° and 19.5° 2θ represents the crystalline phase [30], while the shoulder represents the non-crystalline (amorphous) part of PVA sample. The large peak at $2\theta = 19.5°$ corresponds to (110) reflection, a plane which contains the extended planar zig-zag chain direction of the crystallites. The 90/10 wt% PVA/PEG blend exhibit only an amorphous scattering peak and the broad peak of PVA centered at $2\theta = 19.5°$ diminished nearly. It should be noticeable that the (110) diffraction of PVA crystal is due to the intermolecular interference between PVA chains in the direction of the intermolecular hydrogen bonding. Further investigation of XRD for different PVA/PEG blends illustrated that the main peak at $2\theta = 19.5$ decreased gradually with increasing of PEG content. In addition, the decrease in the intensity of the (110) diffraction corresponds to the decrease in the number of PVA chains packing together, resulting in a larger size crystallite in PVA blend, and this indicates that the crystalline phase of PVA structure is suppressed. The factor that may affect PVA crystalline behavior is due to blending with PEG. Hence, a nearly amorphous or a lower crystalline 90/10 PVA/PEG must have a heterogeneous and thinner network structure.
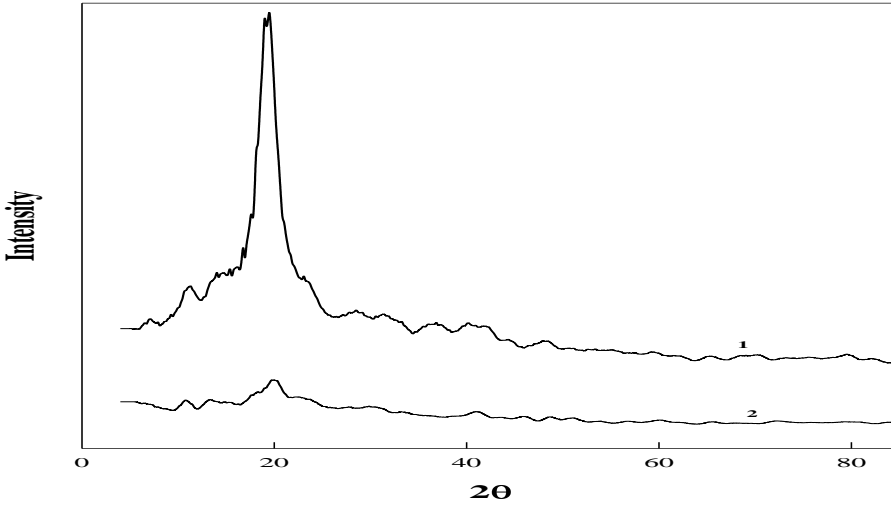
Fig. 5. X-ray diffraction patterns of unirradiated PVA (1) and PVA/PEG (90/10 wt%) blend (2).

Analysis of positions and shape of diffraction peaks provides with knowledge about interplanar spacing (d) and crystalline percent (X_c %). The d spacing is usually estimated using Bragg's equation:

$$n\lambda = 2d \sin \theta \tag{6}$$

where, λ is the X-ray wavelength, n integer number, and θ is the angle of deviation of the diffracted beam. The crystallinity percent of samples was estimated from the ratio of the integrated intensity of peak associated with crystalline reflections to the total integrated area of the spectrum, i.e.

$$X_c = I_C/I_T \tag{7}$$

where X_c is the crystalline fraction, and I_C and I_T are the crystalline and total integrated intensities, respectively.

The calculated values of *d* spacing and crystallinity percentage (X_c %) are listed in Table 2. The crystallinity percentage of PVA was calculated on the basis of changes in the main crystalline peak at 19.5°. One can see that the crystallinity percent of both PVA and PVA/PEG (90/10 wt%) samples decrease with increasing irradiation dose. Also, the level of X_c values for PVA/PEG blends is lower than that for PVA sample. The blending of PVA with PEG decreases chain mobility due to strong interaction between blend components. This behavior results in a decrease in crystal growth rate which in turn reduce the crystallinity percentage. In addition, the interplanar spacing (*d*) was found to decrease with increasing irradiation dose. The decreasing behavior in both crystallinity percent and d spacing of PVA and PVA/PEG samples can be attributed to the increasing

of radiation induced crosslinking which implies a presence of strain on crystals as a result of the formation of three dimensional network chain structures.

Table 2. Calculated crystallinity and *d*-spacing of PVA and PVA/PEG (90/10 wt%) samples.

Dose, kGy	PVA		PVA/PEG (90/10 wt%)	
	(X_c %)	*d*-spacing, Å	(X_c %)	*d*-spacing, Å
0.0	45	4.55	29	4.48
50	42	4.52	24	4.44
100	39	4.50	20	4.41

3.4. *Differential scanning calorimetry (DSC)*

It is well known that glass transition temperature (T_g) of a polymer blend is one of the most important criteria for the miscibility of its components. PVA polymer has a glass transition at about 83°C and a melting point at 225°C [31]. Fig. 6 shows DSC thermograms of unirradiated PVA and PVA/PEG blends. For PVA sample, a broad peak centered around 120°C represents the evaporation of residual water, and a sharp peak at approximately 226°C represents the melting of PVA. It can be seen that the PVA/PEG blends have two endothermic peaks beside the broad peak at about 100-110°C. The new endothermic peak for PVA/PEG blend appeared within the temperature range 50-60°C, and the maximum of this peak was found to increase with increasing of PEG content. Since PEG crystallizes under the given condition, this peak may arise from the melting of PEG component. The existence of the two melting points for PVA/PEG blend revealed the occurrence of two kinds of crystal domains for PVA and PEG components.

   Two glass transition temperatures can be identified for PVA/PEG, (90/19 wt%) blend at 47°C and 81°C assigned for PEG and PVA components, respectively (Fig. 6). For higher compositions of PEG, only one T_g appears which is ascribed to PVA component. It seems that the glass transition temperature for higher PEG content is weak or too broad to measure. One can see that the melting point of PVA decreases with increasing PEG content. This is opposite to the behavior of PEG melting point which is increased with increasing of PEG content. It is thought here that blending PVA with PEG decreases both crystallization rate of PVA and crystals formation during quenching process, resulting in more amorphous content. Also, the increase of PEG content resulted in an increase of PEG crystallization and in sequence increase the melting of PEG. Moreover, it was found that the T_g and T_m decrease as a function of increasing irradiation dose. The extent of decrease in T_g or T_m increases as a result of irradiation (see Table 3).
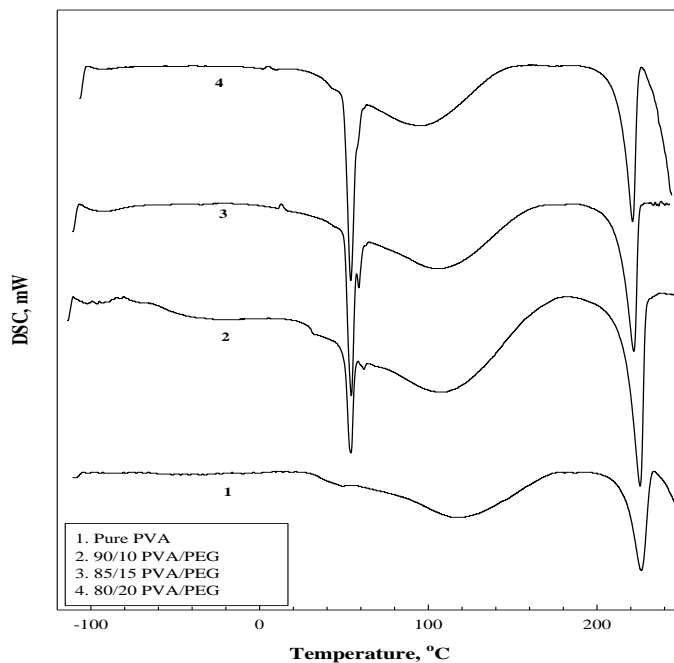
Fig. 6.   DSC thermograms of unirradiated PVA and its different blends with various PEG contents.

Table 3.   Glass transition temperature (T_g), melting point (T_m) and crystallinity percent (X_c) of PVA and PVA/PEG blends.

dose, kGy	sample	T_g °C	T_m °C	X_c %
0		83	227	52.5
75	PVA	79	224	49.6
100		79	215	46.5
0		81	226	48.3
75	PVA/PEG (90/10 wt%)	79	220	49.5
100		78	213	45.7
0		78	223	31.9
75	PVA/PEG (85/15 wt%)	77	217	30.5
100		77	216	28.8
0		76	222	26.8
75	PVA/PEG (80/20 wt%)	74	216	21.8
100		73	211	21.5

The DSC parameters and degree of crystallinity for PVA and PVA/PEG samples are summarized in Table 3. It was found that the degree of crystallinity of PVA decreases with increasing either PEG content or irradiation dose. The decrease of crystallinity with irradiation can be correlated with the behavior of melting point decrease with irradiation, suggesting that crystallinity and perfection of crystal structures were reduced as a result of increasing degree crosslinking. It is well known that, the arrangement of molecular chains from irregular to regular is essential for crystallization, and molecular chains have a tendency to move into the crystal lattice. Overloading PEG component may delay the onset of crystallization and decrease the crystallinity as a whole partly due to reduction of PVA chain mobility and physical interaction (hydrogen bonding) between PVA and PEG, i.e. PEG component serves as plasticizer which in turn suppresses and/or delay the crystallization process (crystallinity percent).

4. Conclusion

The main conclusions of the present work can be summarized as follows:

    a. The swelling ratio gradually decreases with the increase of irradiation dose whereas the gel content % (i.e., crosslink density) increased markedly with increasing irradiation dose.

    b. The increase of PEG content onto PVA matrix increases swelling ratios and on the hand gel content decreased markedly with increasing PEG content.

    c. The decrease in 1133 cm^{-1} absorption peak intensity can be attributed due to increase of PEG content and this reflects the negative role of the PEG on the crystalline nature of the PVA.

    d. XRD shows that blending PVA with PEG leads to a decrease in chain mobility in matrix structure due to strong interaction between blend components. This behavior results in a decrease in crystal growth rate which in turn reduces crystallinity percentage.

    e. From the viewpoint of thermodynamics, the existence of specific interactions, such as hydrogen bonding and polar interaction, between blend components could induce miscibility.

    f. DSC data show that T_m, T_g, and crystallinity percentage decrease as a result of irradiation and also due to blending of PVA matrix with PEG. The extent of decrease in DSC parameters increases with increasing either irradiation dose or the PEG content.

References

1. S. G. Abd Alla, H. M. Nizam El-Din, and A. M. El-Naggar, J. Appl. Polym. Sci. **102**, 1129 (2006). http://dx.doi.org/10.1002/app.24370
2. K. M. Abd El-Kader, A. M. Y. El-Lawindy, A. F. Mansour, and S. F. Abd Hamied, J. Appl. Polym. Sci. **84**, 1295 (2002). http://dx.doi.org/10.1002/app.10486
3. K. M. Abd El-Kader and A. S. Orabi, Polym. Testing **21**, 591 (2002). http://dx.doi.org/10.1016/S0142-9418(01)00129-5

4.   K. M. Abd El-Kader and S. F. Abdel Hamied, J. Appl. Polym. Sci. **86**, 1219 (2002).
     http://dx.doi.org/10.1002/app.11068
5.   K. M. Abd El-Kader, S. F. Abd Hamied, A. B. Mansour, A. M. El-Lawindy, and F. El-Tantaway, Polym. Testing **21**, 849 (2002).
6.   M. Sato, T. Koshino, Y. Kajitani, I. Inamura, and Y. Kubo, J. Appl. Polym. Sci. **93**, 1616 (2004). http://dx.doi.org/10.1002/app.20610
7.   Y. Dog, V. Niholy, and M. J. Jean, Macromolecules **32** (16), 518 (1999).
8.   M. Teresa and R. G. Adilson, A. Pessoa, Polym. Int. **50**, 1068 (2001).
     http://dx.doi.org/10.1002/pi.745
9.   M. Barsbay and A. Gunner, J. Appl. Polym. Sci. **100**, 4587 (2006).
     http://dx.doi.org/10.1002/app.22797
10. M. A. De Ilarduya, J. L. Euiburu, E. Espi, J. J. Iruin, and M. J. Fernandez-Berridi, Macromol. Chem. Phys. **194**, 501 (1993). http://dx.doi.org/10.1002/macp.1993.021940213
11. M. R. Landry, D. J. Massa, C. J. T. Landry, D. M. Teegarden, R. H. Colby, T. E. Long, and P. M. Henrichs, J. Appl. Polym. Sci. **54**, 991 (1994).
     http://dx.doi.org/10.1002/app.1994.070540801
12. W. Chen and J. Wu, M. Jiang, Macromol. Chem. Phys. **199**, 1683 (1998).
     http://dx.doi.org/10.1002/(SICI)1521-3935(19980801)199:8<1683::AID-MACP1683>3.0.CO;2-O
13. I. G. Martin, K. H. Roleister, R. Rosenau, and R. Koningsveld, J. Polym. Sci. Part B: Polym. Phys. **24**, 723, (1986). http://dx.doi.org/10.1002/polb.1986.090240401
14. M. M. Colemanm and P. C. Painter, Appl. Spectrosc. Rev. **23**, 255 (1984).
     http://dx.doi.org/10.1080/05704928408060422
15. M. Song and F. Long, Eur. Polym. J. **27**, 983 (1991).
     http://dx.doi.org/10.1016/0014-3057(91)90045-P
16. C. M. Hassan and N. A. Peppas, Macromolecules **33**, 2472 (2000).
     http://dx.doi.org/10.1021/ma9907587
17. N. A. Peppas and D. Tennenhouse, J. drug Del. Sci. Tech. **14** (4), 291 (2004).
18. R. F. T. Stepto, Polymer Networks; Wiley: Chichester, England, **72**, (1998).
19. C. T. Ratnam and K. Zaman, Angew. Macromol. Chem. **269**, 42 (1999).
     http://dx.doi.org/10.1002/(SICI)1522-9505(19990801)269:1<42::AID-APMC42>3.0.CO;2-K
20. J. M. Rosiak, Radiat. Phys. Chem., **51** (1), 13 (1998).
     http://dx.doi.org/10.1016/S0969-806X(97)00254-5
21. M. Shibayama, T. Yamamoto, C. F. Xiao, S. Sation kurai, A. Hayama, and S. Nomura, Polymer **32**, 1010 (1991). http://dx.doi.org/10.1016/0032-3861(91)90586-8
22. R. T Morrison and R. N. Boyd, Organic chemistry, 6th ed. (Prentice-Hall, New Jersey, 1992) **36**, 3089.
23. A. S. Orabi, Montatsh Chem. **129**, 1139 (1998).
24. R. Jayasekara, I. Harding, I. Bowater, G. B. Y Christie, G. T. Lonergan, Polym. Test. **23**, 17 (2004). http://dx.doi.org/10.1016/S0142-9418(03)00049-7
25. A. K. Abd El-Kader, J. Appl. Polym. Sci. **88**, 589 (2003). http://dx.doi.org/10.1002/app.11743
26. H. Tadokoro, Bull. Chem. Soc. Jpn. **32**, 1252 (1959). http://dx.doi.org/10.1246/bcsj.32.1252
27. H. Tadokoro, S. Seki, I. Mita, Bull. Chem. Soc. Jpn. **28**, 559 (1955).
     http://dx.doi.org/10.1246/bcsj.28.559
28. N. A. Peppas, E. Merrill, J. Polym. Sci., **14**, 441 (1976).
29. M. Ma, H. Wu, C. Lee, J. Poly. Sci: Part B: Polym Physics **36**, 1721 (1998).
     http://dx.doi.org/10.1002/(SICI)1099-0488(19980730)36:10<1721::AID-POLB13>3.0.CO;2-B
30. P. Hong, J. Chen, H. Wu, J. Appl. Polym. Sci. **69**, 2477 (1998).
     http://dx.doi.org/10.1002/(SICI)1097-4628(19980919)69:12<2477::AID-APP19>3.0.CO;2-U
31. S. C Chen, X. L. Wang, Y. Z. Wang, K. K. Yang, Z. X. Zhou, G. Wu, J. Biomed. Mater Res. **80**A (2), 453 (2007). http://dx.doi.org/10.1002/jbm.a.30938   PMid:17013860
32. N. V. Bhat, M. M. Nate, V. A Bambole, M. B. Kurup, J. Appl. Polym. Sci. **98**, 276 (2005).
     http://dx.doi.org/10.1002/app.21999